Published in final edited form as:
Science. 2011 April 15; 332(6027): 358–361. doi:10.1126/science.1192149.

Noncanonical TGFβ Signaling Contributes to Aortic Aneurysm Progression in Marfan Syndrome Mice

Tammy M. Holm[1,*], **Jennifer P. Habashi**[1,2,*], **Jefferson J. Doyle**[1,*], **Djahida Bedja**[3], **YiChun Chen**[1], **Christel van Erp**[1], **Mark E. Lindsay**[1,2], **David Kim**[1], **Florian Schoenhoff**[1], **Ronald D. Cohn**[1,2], **Bart L. Loeys**[4], **Craig J. Thomas**[5], **Samarjit Patnaik**[5], **Juan J. Marugan**[5], **Daniel P. Judge**[6], and **Harry C. Dietz**[1,2,6,†]

[1] Howard Hughes Medical Institute and Institute of Genetic Medicine, Johns Hopkins University School of Medicine, Baltimore, MD 21205, USA

[2] Division of Pediatric Cardiology, Department of Pediatrics, Johns Hopkins University School of Medicine, Baltimore, MD 21205, USA

[3] Department of Molecular and Comparative Pathobiology, Johns Hopkins University School of Medicine, Baltimore, MD 21205, USA

[4] Centre for Medical Genetics, Ghent University, 9000 Ghent, Belgium

[5] National Institutes of Health Chemical Genomics Center, Rockville, MD 20850, USA

[6] Department of Medicine, Johns Hopkins University School of Medicine, Baltimore, MD 21205, USA

Abstract

Transforming growth factor–β (TGFβ) signaling drives aneurysm progression in multiple disorders, including Marfan syndrome (MFS), and therapies that inhibit this signaling cascade are in clinical trials. TGFβ can stimulate multiple intracellular signaling pathways, but it is unclear which of these pathways drives aortic disease and, when inhibited, which result in disease amelioration. Here we show that extracellular signal–regulated kinase (ERK) 1 and 2 and Smad2 are activated in a mouse model of MFS, and both are inhibited by therapies directed against TGFβ. Whereas selective inhibition of ERK1/2 activation ameliorated aortic growth, Smad4 deficiency exacerbated aortic disease and caused premature death in MFS mice. Smad4-deficient MFS mice uniquely showed activation of Jun N-terminal kinase–1 (JNK1), and a JNK antagonist ameliorated aortic growth in MFS mice that lacked or retained full Smad4 expression. Thus, noncanonical (Smad-independent) TGFβ signaling is a prominent driver of aortic disease in MFS mice, and inhibition of the ERK1/2 or JNK1 pathways is a potential therapeutic strategy for the disease.

The transforming growth factor–β (TGFβ) ligands belong to a family of cytokines that regulates diverse cellular functions, including proliferation, differentiation, and synthetic repertoire. TGFβ is secreted from cells as part of a large latent complex that binds to extracellular matrix (ECM) proteins including fibrillin-1 (1), the deficient gene product in

†To whom correspondence should be addressed. hdietz@jhmi.edu.
*These authors contributed equally to this work.

Supporting Online Material
www.sciencemag.org/cgi/content/full/332/6027/358/DC1
Materials and Methods
Figs. S1 to S7
References

Marfan syndrome (MFS). Current models posit that ECM sequestration of TGFβ inhibits its activation, thereby limiting its ability to stimulate cell surface receptors, TβRI and TβRII (2, 3). In canonical signaling, the TβRI/II complex phosphorylates receptor-activated Smad2 and/or Smad3 (to pSmad2 and pSmad3, respectively), which leads to recruitment of Smad4, translocation to the nucleus, and the transcription of Smad-dependent genes (4). Recent work has shown that TGFβ also induces other (noncanonical) pathways, including the RhoA and mitogen-activated protein kinase (MAPK) cascades, the latter of which includes extracellular signal–regulated kinase (ERK), Jun N-terminal kinase (JNK), and p38 (5–7). TGFβ activates these by phosphorylation to pERK, pJNK, and pp38, respectively. In light of these findings, the exclusive focus on Smad signaling in TGFβ-related pathogenetic models needs to be reconsidered.

Increased Smad2/3 activation and increased expression of Smad-responsive genes (e.g., connective tissue growth factor and plasminogen-activator inhibitor–1, PAI-1) have been observed in the lung, skeletal muscle, mitral valve, and aortic wall in humans and a mouse model of MFS (8–11). Treatment of MFS mice with TGFβ-neutralizing antibody (TGFβNAb) ameliorates the phenotype in all of these tissues, in association with attenuated pSmad2/3 signaling (8–11). A similar rescue is achieved by using the angiotensin II type 1 receptor–blocker losartan (8–11), which is known to reduce the expression of TGFβ ligands, receptors, and activators (12–14). It has also been shown that mutations in TβRI or II, which lead to a paradoxical increase in pSmad2 signaling in the aortic wall, cause Loeys-Dietz syndrome, a condition that has considerable phenotypic overlap with MFS, including aortic aneurysm (15, 16). Together, these earlier observations suggested that canonical TGFβ signaling drives disease pathogenesis in MFS. We have now explored the relative contributions of canonical and noncanonical TGFβ signaling cascades in MFS mice, by either genetically or pharmacologically inhibiting each cascade and analyzing the resultant phenotypic consequences.

We performed Western blot analysis on the proximal ascending aorta of 12-month-old mice heterozygous for a missense mutation in *Fbn1* (*Fbn1*$^{C1039G/+}$), a validated animal model of MFS (17). Compared with wild-type (WT) littermates, *Fbn1*$^{C1039G/+}$ mice showed a significant increase in activation of Smad2, ERK1/2, and MAPK kinase 1 (MEK1), the upstream activator of ERK1/2 ($P < 0.05$, $P < 0.001$, and $P < 0.05$, respectively) (Fig. 1A). In contrast, there was no difference in the activation of Smad3; JNK1; p38; ERK5; Rho-associated coiled-coil containing protein kinase–1 (ROCK1); or LIMK1, a downstream target of ROCK1 (Fig. 1A and fig. S1) (18). Furthermore, an in vivo trial of fasudil, a well-established inhibitor of the RhoA/ROCK pathway [details discussed in (18)] failed to attenuate aortic root growth in *Fbn1*$^{C1039G/+}$ mice (fig. S2).

Because TGFβNAb and losartan attenuate aortic root growth in *Fbn1*$^{C1039G/+}$ mice (fig. S3) (10), if Smad2 or ERK1/2 are important mediators of aortic disease in MFS, one would expect their activation to be reduced by these agents. Prior work demonstrated that Smad2 activation is decreased by both therapies (10). We now find that compared with placebo-treated littermates, *Fbn1*$^{C1039G/+}$ mice treated with either TGFβNAb or losartan also show a significant reduction in ERK1/2 activation ($P < 0.01$ for both) (Fig. 1B).

To confirm that ERK1/2 is a driver, rather than simply a marker, of aortic aneurysm progression, 2-month-old *Fbn1*$^{C1039G/+}$ mice were treated for 2 months with the selective MEK1/2 inhibitor RDEA119 (19). Aortic root size was measured by echocardiography at 2 months (baseline before treatment) and 4 months of age (Fig. 1C). Aortic root growth was significantly greater in placebo-treated *Fbn1*$^{C1039G/+}$ mice, compared with WT littermates ($P < 0.05$). Aortic root growth in RDEA119-treated *Fbn1*$^{C1039G/+}$ mice was significantly less than that of placebo-treated *Fbn1*$^{C1039G/+}$ littermates ($P < 0.01$) and indistinguishable

from that observed in WT mice ($P = 0.15$). RDEA119 therapy had no significant effect in WT mice ($P = 0.24$), which illustrated that inhibition of ERK1/2 activation specifically targets MFS-associated pathological aortic root growth, while still allowing for normal physiological growth.

The specificity of RDEA119 was confirmed by Western blot analysis of the proximal ascending aorta. Compared with placebo-treated *Fbn1*$^{C1039G/+}$ littermates, RDEA119-treated *Fbn1*$^{C1039G/+}$ mice showed a significant reduction in ERK1/2 activation ($P < 0.01$), whereas Smad2, JNK1, p38 and ERK5 activation was unchanged (Fig. 1D). This result also shows that Smad2 activation in *Fbn1*$^{C1039G/+}$ mice is not ERK-dependent. Together, these data suggest that TGFβ-driven ERK1/2 activation contributes to aortic aneurysm progression in MFS mice and that antagonism of this pathway may be therapeutically useful.

To determine whether canonical signaling contributes to aortic disease progression in MFS, we introduced haploinsufficiency for Smad4, a critical mediator of canonical TGFβ signaling, into our MFS mouse model. We bred *Fbn1*$^{C1039G/+}$ mice to mice harboring a deletion of exon 8 of the *Smad4* gene. Homozygosity for this *Smad4* allele (*S4*$^{-/-}$) results in the death of embryos (20). In contrast, haploinsufficient mice (*S4*$^{+/-}$) are fertile, have normal life spans, and show clinically relevant attenuation of Smad-dependent signaling in several tissues, including the stomach, breast, and intestine (20).

The *Fbn1*$^{C1039G/+}$ MFS mouse model shows progressive aortic root dilatation, but does not typically progress to aortic dissection or premature death. Whereas almost all WT, *S4*$^{+/-}$ and *Fbn1*$^{C1039G/+}$ mice survived to 8 months of age, *S4*$^{+/-}$*:Fbn1*$^{C1039G/+}$ mice died prematurely. This was first evident by 1 month of age; by 3 months 40% had died, and by 8 months 70% had died (Fig. 2A). Necropsy of these animals revealed hemothorax and hemopericardium in all cases, indicative of proximal aortic rupture; there was no evidence of aortic rupture in any WT, *S4*$^{+/-}$, or *Fbn1*$^{C1039G/+}$ mice.

Echocardiography at 3 months of age revealed significant enlargement of both the aortic root and the ascending aorta in *S4*$^{+/-}$*:Fbn1*$^{C1039G/+}$ mice, compared with *Fbn1*$^{C1039G/+}$ littermates ($P < 0.0001$ and $P < 0.001$, respectively) (Fig. 2B). These data provide a conservative estimate of the effect of *Smad4* haploinsufficiency, because premature deaths in the *S4*$^{+/-}$*:Fbn1*$^{C1039G/+}$ cohort effectively eliminated more severe cases from the analysis. No difference in aortic root or ascending aortic size was observed between WT and *S4*$^{+/-}$ mice ($P = 0.20$ and $P = 0.20$, respectively) (Fig. 2B), which indicated that the deleterious effect of *Smad4* haploinsufficiency was limited to MFS mice.

After death of the mice, we performed Verhoeff–Van Gieson (VVG) staining of the proximal ascending aorta to assess whether there were any abnormalities in aortic architecture (Fig. 2C). Compared with WT littermates, *Fbn1*$^{C1039G/+}$ mice showed increased aortic medial thickening, elastic fiber fragmentation, and elastic fiber disarray, collectively quantified as an aortic architecture score ($P < 0.0001$) (fig. S4). *S4*$^{+/-}$*:Fbn1*$^{C1039G/+}$ mice showed an exaggeration of these pathologic changes ($P < 0.05$). By contrast, there was no significant difference between WT and *S4*$^{+/-}$mice ($P = 0.94$). The histological changes in the aorta therefore paralleled the echocardiography findings and support the conclusion that *Smad4* haploinsufficiency exacerbates aortic disease in MFS mice.

Using Western blot analysis, we evaluated the effect of *Smad4* haploinsufficiency on canonical and noncanonical TGFβ signaling in the proximal ascending aorta (Fig. 3). As anticipated, *S4*$^{+/-}$and *S4*$^{+/-}$*:Fbn1*$^{C1039G/+}$ mice showed a roughly 50% reduction in expression of Smad4 protein, compared with WT and *Fbn1*$^{C1039G/+}$ mice. Compared with WT animals, *Fbn1*$^{C1039G/+}$ mice showed significantly greater activation of Smad2 and ERK1/2 ($P < 0.01$ and $P < 0.05$, respectively) and a significant increase in expression of the

Smad2-responsive gene product PAI-1 ($P < 0.01$). However, there was no further increase in Smad2 activation, ERK1/2 activation, or PAI-1 expression in $S4^{+/-}$:$Fbn1^{C1039G/+}$ mice ($P = 0.35$, $P = 0.90$, and $P = 0.85$, respectively). This indicates that *Smad4* haploinsufficiency did not attenuate Smad-dependent signaling and that increased Smad2 or ERK1/2 activation could not be invoked as the cause of the aortic disease exacerbation seen in $S4^{+/-}$:$Fbn1^{C1039G/+}$ mice.

We next assessed whether other TGFβ-dependent canonical or noncanonical pathways could account for these changes (Fig. 3). There was no significant difference in Smad3 or p38 activation in WT, $Fbn1^{C1039G/+}$, or $S4^{+/-}$:$Fbn1^{C1039G/+}$ mice. Although there was no significant difference in JNK1 activation between $Fbn1^{C1039G/+}$ and WT mice, $S4^{+/-}$:$Fbn1^{C1039G/+}$ mice demonstrated unique activation of JNK1 ($P < 0.05$). We therefore treated a cohort of $S4^{+/-}$:$Fbn1^{C1039G/+}$ mice with SP600125, a selective JNK inhibitor (21). SP600125 treatment led to a significant reduction in both aortic root and ascending aortic growth in $S4^{+/-}$:$Fbn1^{C1039G/+}$ mice, compared with placebo-treated littermates ($P < 0.001$ and $P < 0.05$, respectively) (Fig. 4A). Furthermore, SP600125 treatment prevented the premature death due to aortic dissection seen in these animals. At 3 months of age, 50% of placebo-treated $S4^{+/-}$:$Fbn1^{C1039G/+}$ mice had died from aortic dissection, whereas all of the SP600125-treated $S4^{+/-}$:$Fbn1^{C1039G/+}$ mice were still alive (Fig. 4B).

Although JNK1 activation is not increased in the aortas of $Fbn1^{C1039G/+}$mice, SP600125 treatment ameliorated their aortic root growth, compared with placebo-treated $Fbn1^{C1039G/+}$ littermates ($P < 0.05$) (Fig. 4A). This correlated with a reduction of JNK1 activation to levels below baseline, whereas ERK1/2 activation remained unaffected, in SP600125-treated $Fbn1^{C1039G/+}$ animals (fig. S5). This observation is consistent with prior work showing that SP600125 can ameliorate abdominal aortic aneurysm induced by the periaortic application of calcium chloride, in association with reduced JNK1 activation (22). These data suggest that both ERK1/2 and JNK1 can contribute to aortic disease in fibrillin-1–deficient mice; whether or not this relies upon downstream cross-talk between these signaling cascades remains to be determined. Taken together, these data further support the conclusion that noncanonical TGFβ signaling is a prominent determinant of aortic aneurysm progression in MFS mice.

ERK activation was recently shown to occur in the aorta of a fibulin-4–deficient mouse model of cutis laxa with aneurysm, although a mechanistic link remains to be elucidated (23). ERK activation also appears to be central to the pathogenesis of cardiovascular disease in Noonan syndrome (24, 25). Although aortic aneurysm has been described in this condition (26, 27), it is not highly penetrant, which suggests as yet undefined context specificity. It is also notable that the combination of aortic root and ascending aortic aneurysm seen in $S4^{+/-}$:$Fbn1^{C1039G/+}$ mice is similar to that observed in individuals with either Loeys-Dietz syndrome or bicuspid aortic valve and aneurysm. Both conditions are associated with increased TGFβ signaling in the aortic wall (15, 28), but the contribution of noncanonical TGFβ signaling cascades has not been revealed.

In summary, this work defines a critical role for noncanonical TGFβ-dependent signaling in aneurysm pathogenesis in MFS mice. It also defines inhibition of ERK1/2 or JNK1 activation as possible therapeutic strategies for MFS and suggests that such therapies may find broader application. Finally, it focuses attention on noncanonical TGFβ signaling cascades in MFS-related conditions, where etiology or pathogenesis remains poorly understood.

Supplementary Material

Refer to Web version on PubMed Central for supplementary material.

Acknowledgments

Supported by the National Institutes of Health (H.C.D. and D.P.J), Howard Hughes Medical Institute (H.C.D.), National Marfan Foundation (H.C.D., J.P.H., and J.J.D.), Cellular and Molecular Medicine Training Program (J.J.D.), National Human Genome Research Institute Intramural Research Program and the NIH Therapeutics for Rare and Neglected Diseases Program (C.J.T., S.P., and J.J.M.), and the Smilow Center for Marfan Syndrome Research (H.C.D.). We thank Dr. C. Deng for the *Smad4*-targeted mice. Johns Hopkins University and the authors (H.C.D., J.P.H., D.P.J., and R.C.) have filed a patent relating to the use of TGFβ antagonists, including angiotensin II type 1 receptor blockers, for the treatment of Marfan syndrome.

References and Notes

1. Isogai Z, et al. J Biol Chem. 2003; 278:2750. [PubMed: 12429738]
2. Dietz HC. J Clin Invest. 2010; 120:403. [PubMed: 20101091]
3. Hynes RO. Science. 2009; 326:1216. [PubMed: 19965464]
4. Kang JS, Liu C, Derynck R. Trends Cell Biol. 2009; 19:385. [PubMed: 19648010]
5. Derynck R, Zhang YE. Nature. 2003; 425:577. [PubMed: 14534577]
6. Lee MK, et al. EMBO J. 2007; 26:3957. [PubMed: 17673906]
7. Yamashita M, et al. Mol Cell. 2008; 31:918. [PubMed: 18922473]
8. Neptune ER, et al. Nat Genet. 2003; 33:407. [PubMed: 12598898]
9. Ng CM, et al. J Clin Invest. 2004; 114:1586. [PubMed: 15546004]
10. Habashi JP, et al. Science. 2006; 312:117. [PubMed: 16601194]
11. Cohn RD, et al. Nat Med. 2007; 13:204. [PubMed: 17237794]
12. Wolf G, Ziyadeh FN, Stahl RA. J Mol Med. 1999; 77:556. [PubMed: 10494801]
13. Fukuda N, et al. Am J Hypertens. 2000; 13:191. [PubMed: 10701820]
14. Naito T, et al. Am J Physiol Renal Physiol. 2004; 286:F278. [PubMed: 14583433]
15. Loeys BL, et al. Nat Genet. 2005; 37:275. [PubMed: 15731757]
16. Loeys BL, et al. N Engl J Med. 2006; 355:788. [PubMed: 16928994]
17. Judge DP, et al. J Clin Invest. 2004; 114:172. [PubMed: 15254584]
18. Materials and methods are available as supporting material on *Science* Online.
19. Iverson C, et al. Cancer Res. 2009; 69:6839. [PubMed: 19706763]
20. Xu X, et al. Oncogene. 2000; 19:1868. [PubMed: 10773876]
21. Bennett BL, et al. Proc Natl Acad Sci USA. 2001; 98:13681. [PubMed: 11717429]
22. Yoshimura K, et al. Nat Med. 2005; 11:1330. [PubMed: 16311603]
23. Huang J, et al. Circ Res. 2010; 106:583. [PubMed: 20019329]
24. Araki T, et al. Nat Med. 2004; 10:849. [PubMed: 15273746]
25. Nakamura T, et al. J Clin Invest. 2007; 117:2123. [PubMed: 17641779]
26. Morgan JM, Coupe MO, Honey M, Miller GA. Eur Heart J. 1989; 10:190. [PubMed: 2924789]
27. Purnell R, Williams I, Von Oppell U, Wood A. Eur J Cardiothorac Surg. 2005; 28:346. [PubMed: 15964762]
28. Gomez D, et al. J Pathol. 2009; 218:131. [PubMed: 19224541]

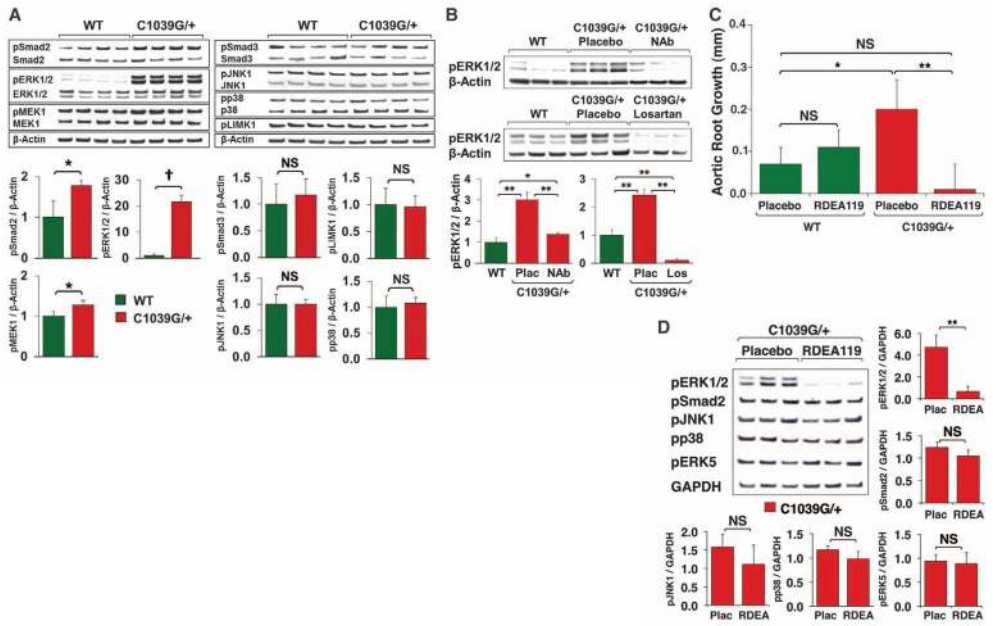

Fig. 1.

Canonical and noncanonical TGFβ signaling in the proximal ascending aorta. (**A**) Western blot analysis of 4 WT and *Fbn1*$^{C1039G/+}$ mice. Note that only pSmad2, pERK1/2, and pMEK1 signaling are increased in *Fbn1*$^{C1039G/+}$ mice. The graphs show normalization to β-actin, but the same outcomes were observed with normalization to the respective total proteins. (**B**) Western blot analysis of three each of WT and of *Fbn1*$^{C1039G/+}$ mice treated with placebo, TGFβNAb, or losartan. Note the significant reduction in pERK1/2 signaling after treatment with TGFβNAb (NAb) or losartan (Los). (**C**) Aortic root growth in placebo-treated WT ($n = 5$), placebo-treated *Fbn1*$^{C1039G/+}$ ($n = 6$), RDEA119-treated WT ($n = 3$), and RDEA119-treated *Fbn1*$^{C1039G/+}$ ($n = 7$) mice. Note that RDEA119 therapy selectively reduced growth in *Fbn1*$^{C1039G/+}$ mice. Final absolute aortic root diameter (mm): WT (1.62 ± 0.08), placebo-treated *Fbn1*$^{C1039G/+}$ (2.15 ± 0.17), RDEA119-treated WT (1.64 ± 0.09), RDEA119-treated *Fbn1*$^{C1039G/+}$ (1.94 ± 0.07). (**D**) Western blot analysis of three placebo- and three RDEA119-treated *Fbn1*$^{C1039G/+}$ mice, showing a selective reduction in pERK1/2 signaling in RDEA119-treated mice. Plac, placebo. Values are means ± 2SEM. *$P < 0.05$; **$P < 0.01$; †$P < 0.001$; NS, not significant.

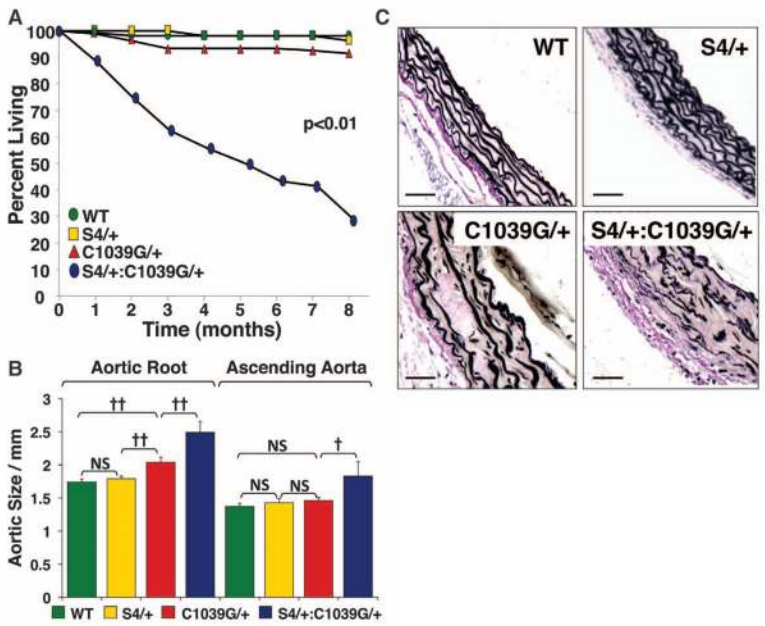

Fig. 2.

Effect of *Smad4* haploinsufficiency ($S4^{+/-}$) on aortic phenotype. (**A**) Survival curve of WT ($n = 112$), $S4^{+/-}$ ($n = 56$), $Fbn1^{C1039G/+}$ ($n = 107$) and $S4^{+/-}$:$Fbn1^{C1039G/+}$ ($n = 85$) mice. Note the high rate of premature death due to aortic dissection in $S4^{+/-}$:$Fbn1^{C1039G/+}$ mice. (**B**) Aortic root and ascending aortic diameter, measured by echocardiography, at 3 months of age in WT ($n = 9$), $S4^{+/-}$ ($n = 11$), $Fbn1^{C1039G/+}$ ($n = 24$), and $S4^{+/-}$:$Fbn1^{C1039G/+}$ ($n = 26$) mice. Although $Fbn1^{C1039G/+}$ mice showed a selective increase in aortic root diameter compared with WT littermates, $S4^{+/-}$:$Fbn1^{C1039G/+}$ mice demonstrated an increase in both aortic root and ascending aortic diameter, compared with all other genotypes. (**C**) VVG staining of representative sections of the proximal ascending aorta. Compared with WT littermates, $Fbn1^{C1039G/+}$ mice demonstrated medial thickening and elastic fiber fragmentation, both of which are exacerbated in $S4^{+/-}$:$Fbn1^{C1039G/+}$ mice. Values are means ± 2 SEM. †$P < 0.001$; ††$P < 0.0001$; NS, not significant.

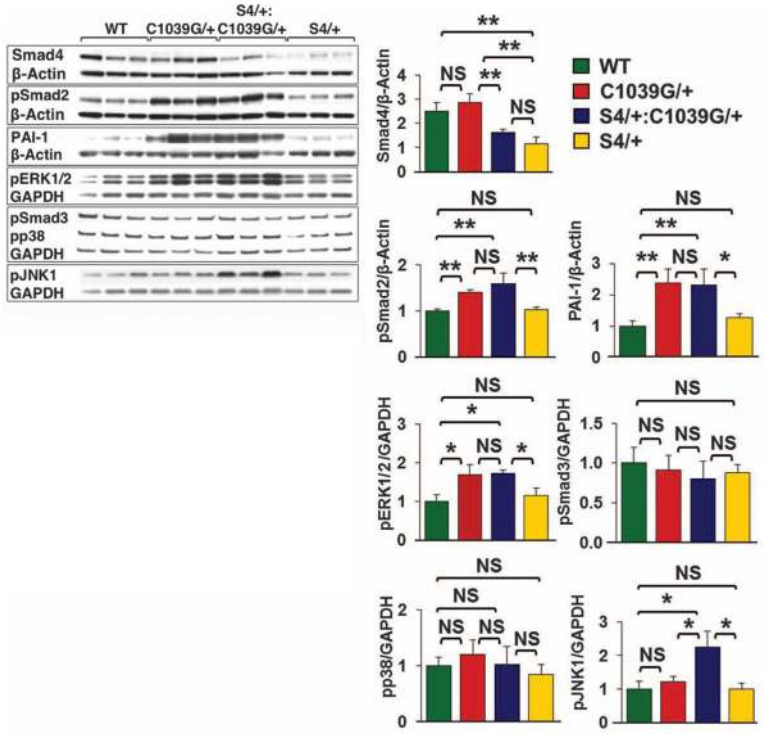

Fig. 3.

Effect of *Smad4* haploinsufficiency ($S4^{+/-}$) on aortic signaling. Western blot analysis of the proximal ascending aorta in three mice each: WT, $S4^{+/-}$, $Fbn1^{C1039G/+}$, and $S4^{+/-}$:$Fbn1^{C1039G/+}$. Note the unique activation of JNK1 in $S4^{+/-}$:$Fbn1^{C1039G/+}$ mice compared with all other genotypes. Values are means ± 2 SEM. *$P < 0.05$; **$P < 0.01$; NS, not significant.

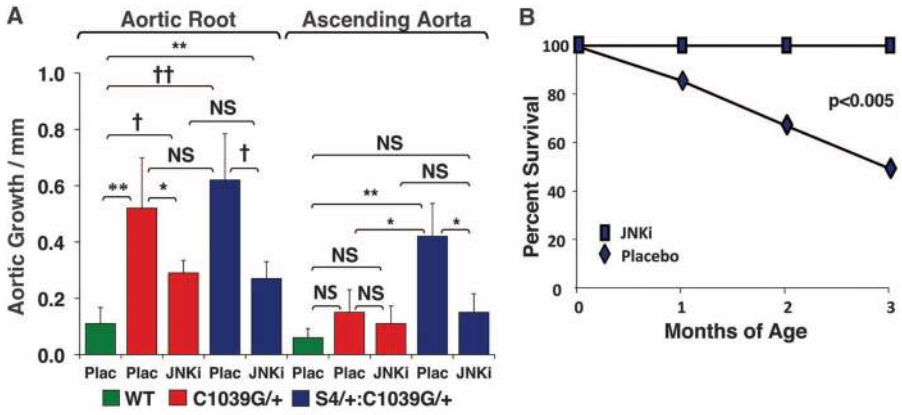

Fig. 4.

Effect of JNK antagonism in the presence of SP600125. (**A**) Aortic root and ascending aortic growth, as measured by echocardiography, in WT mice ($n = 6$) and $Fbn1^{C1039G/+}$ placebo- ($n = 5$) or SP600125-treated ($n = 5$) mice, as well as placebo- ($n = 8$) or SP600125-treated ($n = 11$) $S4^{+/-}$:$Fbn1^{C1039G/+}$ littermates. Note that JNK inhibition decreased aortic root growth in $S4^{+/-}$:$Fbn1^{C1039G/+}$ and $Fbn1^{C1039G/+}$ mice and reduced ascending aortic growth in $S4^{+/-}$:$Fbn1^{C1039G/+}$ mice. Final absolute aortic root and ascending aortic diameter (mm): WT (1.66 ± 0.06; 1.33 ± 0.06), placebo- (2.31 ± 0.02; 1.43 ± 0.10) or SP600125-treated (1.97 ± 0.16; 1.38 ± 0.06) $Fbn1^{C1039G/+}$ mice, placebo- (2.33 ± 0.38; 1.85 ± 0.37) or SP600125-treated (2.09 ± 0.16; 1.47 ± 0.14) $S4^{+/-}$:$Fbn1^{C1039G/+}$ mice. (**B**) Survival curve for $S4^{+/-}$:$Fbn1^{C1039G/+}$ mice treated with either placebo ($n = 8$) or SP600125 ($n = 11$), showing prevention of premature death in SP600125-treated animals. JNKi, JNK inhibitor SP600125; Plac, placebo. Values are means ± 2 SEM. *$P < 0.05$; **$P < 0.01$; †$P < 0.001$; ††$P < 0.0001$; NS, not significant.